JOURNAL OF SPACECRAFT AND ROCKETS
Vol. 44, No. 4, July–August 2007

Building Interplanetary Trajectories with Multiple Gravity-Assisted Maneuvers

Dmitry M. Pisarevsky*
Technion–Israel Institute of Technology, 32000 Haifa, Israel
Alexander Kogan†
Asher Space Research Institute, 32000 Haifa, Israel
and
Moshe Guelman‡
Technion–Israel Institute of Technology, 32000 Haifa, Israel

DOI: 10.2514/1.27888

This paper presents a new method for building gravity-assisted, interplanetary trajectories. Generally, designing interplanetary trajectories using multiple gravity-assisted maneuvers is extremely difficult, due to close approaches to singularities. Numerical implementation faces strong computational instabilities, which often make the solution unfeasible. Furthermore, related optimization problems usually admit a number of local extrema, thus making the overall phase space structure too complex for numerical analysis. The proposed method for building interplanetary trajectories with multiple gravity-assisted maneuvers is based on the concatenation of repeated short sequences of Keplerian arcs, referred to as blocks. These blocks differ from each other only in inclination. The method is applicable to any resonant planetary system counting an arbitrary number of planets in circular or elliptical orbits and allows the assembling of long trajectories otherwise not amenable to computation. The proposed method is presented along with a number of representative examples.

Nomenclature

a	=	semimajor axis, km
h_p	=	altitude at periapsis of hyperbolic passage, km
i	=	inclination angle, rad
J	=	Jacobi's integral value, km^2/s^2
m	=	number of spacecraft's semirevolutions
n	=	number of planet's semirevolutions
p	=	semilatus rectum, km
R_{pl}	=	equatorial radius of flyby planet, km
r	=	distance of the secondary massive body from the central body, km
T	=	orbital period of spacecraft, s
T_{pl}	=	orbital period of planet, s
t	=	time, s
$\boldsymbol{V}$	=	spacecraft's velocity vector, km/s
V_r	=	spacecraft's radial velocity component, km/s
V_θ	=	spacecraft's transversal velocity component, km/s
$\boldsymbol{V}_{pl}$	=	planet's velocity vector, km/s
$V_{pl,r}$	=	planet's radial velocity component, km/s
$V_{pl,\theta}$	=	planet's transversal velocity component, km/s
$\boldsymbol{V}_\infty$	=	relative velocity vector, km/s
V_∞	=	relative velocity magnitude, km/s
δ	=	deflection angle of relative velocity during flyby, rad
θ_{LON}	=	angle between the line of nodes and planet's apsidal line, rad
θ_{AB}	=	relative angle between planet A and planet B, rad
μ	=	gravity constant, km^3/s^2
μ_{pl}	=	gravity constant of flyby planet, km^3/s^2

Received 18 September 2006; revision received 12 March 2007; accepted for publication 18 March 2007.

*Doctoral Student, Faculty of Aerospace Engineering; aedmitry@techunix.technion.ac.il.

†Senior Scientist, Asher Space Research Institute; akogan@techunix.technion.ac.il.

‡Professor, Faculty of Aerospace Engineering; aerglmn@aerodyne.technion.ac.il. Senior Member AIAA.

I. Introduction

GRAVITY-ASSISTED maneuvering is a powerful tool that enables otherwise unaffordable deep space missions. Many well-known missions such as Voyager [1], Galileo [2], and Cassini [3] used gravity-assisted trajectories. NASA launched the twin spacecraft Voyager 1 and Voyager 2 in 1977. This mission was designed to take advantage of a rare geometric arrangement of the outer planets, which allowed a four-planet tour for a minimum propellant and trip time. The formation of Jupiter, Saturn, Uranus, and Neptune allowed the spacecraft to swing from one planet to the other using the gravity-assist technique.

Gravity-assisted maneuver (GAM) theory has been studied for further application in space research. Some recent works about GAM planning are itemized next. Miller and Weeks [4] studied the simplest missions with only one GAM. A spacecraft (s/c) uses gravitational attraction of an intermediate planet to increase the orbital energy and thus is able to reach the destination planet. The paper describes a procedure for finding the launch times, intermediate and destination planet arrivals using Lambert's theorem and a version of Tisserand's criterion to identify the sequence of planets to approach. In [5], Strange and Longuski proposed a graphic method for solving the ballistic problems with GAM based on the graphical use of Tisserand's criterion, without taking into account the synchronization problem. Gravity-assisted trajectories to Jupiter with launch dates between 1999 and 2031 were identified using patched-conic techniques [6]. To identify possible transfers, the authors use the STOUR (Satellite Tour Design Program [7]). The interest was in low launch energy trajectories with low total ΔV and with reasonable time of flight (TOF). Also, for selected cases, the ΔV-optimal solutions were found using the Jet Propulsion Laboratory (JPL) MIDAS (Mission Analysis and Design Software [8]) software package.

However, the design of multi-GAM trajectories is still very far from being routine; every such trajectory is custom-made. This is even more so for trajectories combining GAMs with reactive thrust. For this reason, all algorithms developed until now are limited to relatively small numbers of GAMs. This work is intended to improve

the situation. It proposes a comprehensive, regular class of multi-GAM trajectories, extensive enough to meet the requirements of a variety of interplanetary missions. These trajectories contain only non-coplanar arcs and therefore the transfer angles are $k\pi$, where k is a natural number. This restriction may increase the TOF as compared with the general case. However, this disadvantage is outweighed by the simplicity of the design of very long multi-GAM trajectories, otherwise unmanageable.

Design of interplanetary trajectories often deals with Jacobi's integral value [9] variation. Generally, the variation can be done in several ways. One of the preferable options is the use of GAMs. A standard approach to design a multi-GAM trajectory is to search for a chain of appropriate orbits, connecting initial and final orbits. Determination of each new orbit in the chain requires the solution of two problems: a J variation problem and a synchronization problem. Synchronous trajectories constitute discrete families, whose symmetries are hidden in the arithmetic properties of the primaries' orbital periods. These families are difficult to find and, as a result, building a trajectory by adding new orbits to the chain is nonintuitive due to severe constraints imposed by the synchronism conditions.

Generally, it is difficult to separate J variation from synchronization problems. In the coupled case, the problems must be solved simultaneously after each GAM. In this paper, a new method will be presented enabling one to split these two problems. Initially, the synchronization problem for the system is solved and the set of appropriate orbits for a chain are obtained. Any orbit from the set can be placed in the chain. Next, the J-variation problem is readily solved using orbits from the set, as obtained in the previous step. It is an approach that makes the process of building the multi-GAM trajectories manageable and comprehensible. It uses only a part of available trajectories, namely those non-coplanar with the plane of primaries' orbits. However, it provides the rates of J variation nearly the same as those obtained from numerical solutions of the coplanar problem. This method is applicable to any elliptic three-body problem (3BP) as well as resonant four-body problems.

II. Problem Definition

In a restricted circular 3BP, the Jacobian integral remains constant along a trajectory. Consequently, serial flybys cannot bring the trajectory outside the five-dimensional hypersurface. A cardinally different situation is encountered in an elliptical 3BP problem [9] or in the problem with more than three bodies (N-body problem). Here the Jacobi integral no longer exists and the trajectory is not attached to a hypersurface in the phase space.

Consider now the N-body problem, where the primary body is the sun, there are $(N-2)$ secondary bodies, the planets, and a massless spacecraft. A first approximation to finding a multi-GAM trajectory from a given initial orbit to a given final orbit is to assume that no more than two bodies' gravitational forces simultaneously affect the motion of the spacecraft. This fact allows splitting the problem into $N-2$ subproblems, where each one of the problems is considered as a 3BP (sun, planet, and s/c). Solutions of these problems can be patched according to certain rules and provide an approximated solution of the N-body problem. Still, even after this simplification, the problem solution remains very complicated.

There is still a lower approximation to solve the N-body problem. An interplanetary multi-gravity-assist trajectory may be approximated by a chain of Keplerian arcs, i.e., patched conics [10,11]. In this case, the resulting trajectories are a chain of arcs that start and end near the planets. Separate arcs are connected obeying a set of *concatenation rules*, which must hold on every GAM: 1) preservation of V_∞, 2) limitation of $\boldsymbol{V}_\infty$ vector turning angle, and 3) synchronization with the secondary bodies' orbital motion.

The first rule results from an approximation of J in the 3BP. The second rule results from a restriction on the minimum altitude above the flyby planet. The third rule results from the requirement that the s/c and the next flyby planet will reach the same position at the same time. All three rules are interlaced, which makes the design process very difficult, mainly due to the third rule.

There is, however, a well-known type of trajectory, for which the design process is straightforward: the case of periodic trajectories [12–14] in the circular four-body problem (C4BP). In this case, after every synodic year the two planets return to their original relative positions. Therefore, it is enough to calculate one trajectory subsequence, with duration equal to any natural number of synodic years, and same J at start and end of the sequence. Unfortunately, this requirement makes the use of these trajectories useless for our purpose. Still, periodic orbits inspired us to look at the possibility of splitting the J-variation and synchronization problems. This splitting will enable, as will be shown, to find a straightforward solution to the problem in any resonant astronomical system. Secondary bodies in resonance return periodically to the same configuration with respect to the inertial space. We will use this fact to build multi-GAMs, non-coplanar trajectories, which will enable J to vary gradually.

Two non-coplanar arcs, with the same semimajor axis, eccentricity, and transfer angle, have the same transfer time. But, if the arcs' inclinations are different, then they will have *different* J values. More generally, any variation in inclination inside a chain produces a variation in J. If the total transfer time is equal to the period or some integer number of periods of the resonant system, then the chain can be repeated with a different inclination without recalculation of the synchronization problem. Variation of a chain inclination leads to variation in J, but *not* in transfer time. Using inclination as a "free parameter" we can vary J until the desired value. After the J variation, by using GAMs near one of the system's planets, the final trajectory can easily be transferred to almost any orbit with the same J such that it complies with the *synchronism condition*.

III. Theoretical Background

A. Characteristics of Non-Coplanar Arcs

All the massive secondary bodies are assumed to be in coplanar motion. In this case, GAMs can only occur on the line of nodes (LON) of the non-coplanar arcs. This restricts the transfer angle of the arcs to $k\pi$, where k is a natural number. If k is an even number, then the arc starts and ends at the same distance from the primary body, i.e., the arc becomes a closed orbit, as shown in Fig. 1. If k is an odd number, then the initial and final distances are defined by the orbital radii of the chosen pair of secondary bodies about the primary body, r_1 and r_2 as shown in Fig. 2 for the elliptical 3BP (E3BP) and C4BP. The semilatus rectum of all possible arcs [11] is

$$p = \frac{2r_1 r_2}{c} \tag{1}$$

where $c = r_1 + r_2$. From Eq. (1), it also follows that the transversal velocities are

$$V_{\theta,j} = \sqrt{\frac{2\mu(c - r_j)}{cr_j}} \tag{2}$$

where $j = 1, 2$, μ is the gravitational constant of the primary body. In addition, radial velocities at both ends of an odd arc are equal in

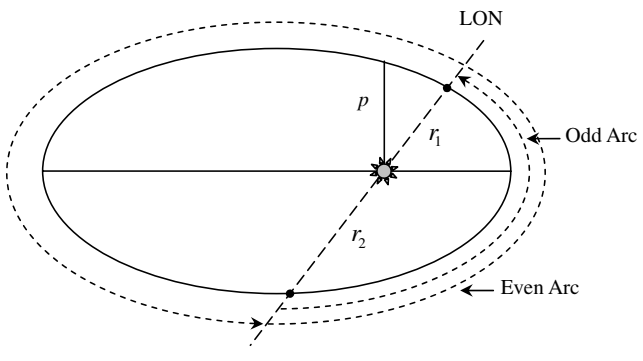

Fig. 1 Odd and even arcs.

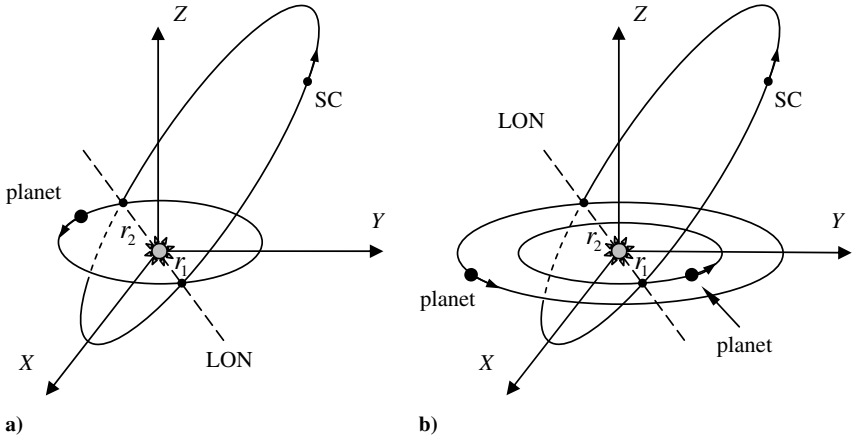

Fig. 2 Geometry of odd arcs in the a) E3BP and b) C4BP.

amplitude but opposite in direction. The radial velocity amplitude at both ends of the arc is given by,

$$V_r = \sqrt{\mu\left(\frac{2}{c} - \frac{1}{a}\right)} \tag{3}$$

Note that contrary to the transversal component, the radial velocity does not need to be the same for all arcs with given ends. It depends on the semimajor axis, which is free. This free parameter will be used next to synchronize the s/c and the secondary bodies.

B. Concatenation of Non-Coplanar Arcs

As was previously stated, a chain of Keplerian arcs approximates a ballistic multi-GAM trajectory. These arcs are linked together according to certain rules. The first rule says two arcs should have equal J. Herein, modulus of the relative velocity,

$$V_\infty^2 = (\boldsymbol{V} - \boldsymbol{V}_{\rm pl}) \cdot (\boldsymbol{V} - \boldsymbol{V}_{\rm pl}) = \boldsymbol{V} \cdot \boldsymbol{V} - 2\boldsymbol{V} \cdot \boldsymbol{V}_{\rm pl} + \boldsymbol{V}_{\rm pl} \cdot \boldsymbol{V}_{\rm pl} \tag{4}$$

can unambiguously replace J.

The spacecraft's and planet's velocity vectors can be obtained by summing the velocity components at their corresponding perifocal frames [15] (see Fig. 3), $\boldsymbol{V} = \boldsymbol{V}_r + \boldsymbol{V}_\theta$, $\boldsymbol{V}_{\rm pl} = \boldsymbol{V}_{{\rm pl},r} + \boldsymbol{V}_{{\rm pl},\theta}$. Thus Eq. (4) transforms into

$$V_\infty^2 = (V_r - V_{{\rm pl},r})^2 + V_\theta^2 + V_{{\rm pl},\theta}^2 - 2V_\theta V_{{\rm pl},\theta} \cos i \tag{5}$$

If the planet's orbit is circular, then $V_{{\rm pl},r} \equiv 0$, $V_{{\rm pl},\theta} \equiv V_{\rm pl}$, and

$$V_\infty^2 = V_r^2 + V_\theta^2 + V_{\rm pl}^2 - 2V_\theta V_{\rm pl} \cos i \tag{6}$$

During each GAM, the magnitude of the relative velocity remains constant (rule 1), however, its direction can change. For a given value of relative velocity magnitude,

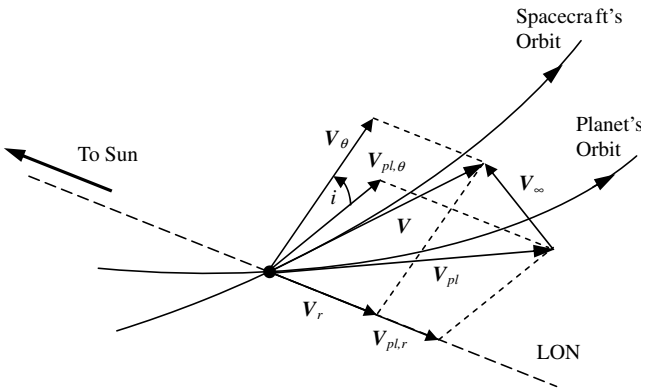

Fig. 3 Velocity diagram at GAM.

$$\boldsymbol{V}_\infty^- \cdot \boldsymbol{V}_\infty^+ = \boldsymbol{V}_\infty^2 \cos\delta \tag{7}$$

where the "−" and "+" superscripts indicate values before and after the GAM, respectively. The left-hand expression of Eq. (7) can be rewritten in the form of

$$\begin{aligned}\boldsymbol{V}_\infty^- \cdot \boldsymbol{V}_\infty^+ &= V_{{\rm pl},r}^2 + V_{{\rm pl},\theta}^2 + V_r^- V_r^+ + V_\theta^- V_\theta^+ \cos\Delta i \\ &\quad - V_{{\rm pl},r}\left(V_r^- + V_r^+\right) - V_{{\rm pl},\theta}\left(V_\theta^- \cos i^- + V_\theta^+ \cos i^+\right)\end{aligned} \tag{8}$$

where $\Delta i \triangleq i^+ - i^-$. The right-hand expression of Eq. (7) is written as

$$V_\infty^2 \cos\delta = \frac{1}{2}\left[\left(V_\infty^-\right)^2 + \left(V_\infty^+\right)^2\right] - 2V_\infty^2 \sin^2\frac{\delta}{2} \tag{9}$$

Equalizing Eqs. (8) and (9), we obtain

$$4V_\infty^2 \sin^2\frac{\delta}{2} = \Delta V_r^2 + \Delta V_\theta^2 + 4V_\theta^- V_\theta^+ \sin^2\frac{\Delta i}{2} \tag{10}$$

where $\Delta V_r \triangleq V_r^+ - V_r^-$ and $\Delta V_\theta \triangleq V_\theta^+ - V_\theta^-$. Now, the only parameter, which controls the deflection δ, is the flyby altitude given by [11],

$$\sin\frac{\delta}{2} = \frac{1}{1 + (R_{\rm pl} + h_p)V_\infty^2/\mu_{\rm pl}} \tag{11}$$

To obtain the flyby altitude as function of the velocity and inclination change during the GAM, we substitute Eq. (10) into Eq. (11). The result is

$$h_p = \frac{\mu_{\rm pl}}{V_\infty^2}\left[2V_\infty\left(\Delta V_r^2 + \Delta V_\theta^2 + 4V_\theta^- V_\theta^+ \sin^2\frac{\Delta i}{2}\right)^{-1/2} - 1\right] - R_{\rm pl} \tag{12}$$

Therefore, two arcs can be patched if $h_p > h_m$, where h_m is the minimal allowed flyby altitude above the planet (rule 2).

C. Synchronism Conditions

In general terms, a synchronism condition establishes a coupling between the angular size of an arc and the respective flight time. Let us denote the first, the second, etc., planets, respectively, by A, B, etc. Their orbital planes are assumed to coincide. Any sequence of these symbols defines a sequence of GAMs, i.e., *an itinerary*. A two-term itinerary is an arc. The {AA}- and {AB}-type arcs are, respectively, *recursive* and *transitional*. Analogously, an itinerary is recursive if it starts and ends near the same planet, otherwise it is transitional.

According to Lambert's theorem, flight time over any arc is

$$t_k = kT + \frac{T}{2\pi}[(\alpha - \sin\alpha) - (\beta - \sin\beta)] \tag{13}$$

Here α and β are defined by

$$r_1 + r_2 + c = 4a\sin^2(\alpha/2), \qquad r_1 + r_2 - c = 4a\sin^2(\beta/2)$$
$$c \triangleq |\mathbf{r}_1 - \mathbf{r}_2| = \sqrt{r_1^2 + r_2^2 - 2r_1 r_2 \cos\theta} \tag{14}$$

Because only non-coplanar arcs are allowed, the spacecraft passes the angle $\theta = m\pi$ over a recursive trajectory. Meanwhile, the departure/arrival planet passes the angle $n\pi$. Obviously, $n \equiv m$ (mod2). Feasible flight times are therefore constrained to a discrete set of values. In particular, the following apply:

1) If $n = 2k$ (even arcs), then $r_1 = r_2$, $c = 0$, and $t_n = nT/2$.

2) If $n = 2k + 1$ (odd arcs), then $c = r_1 + r_2$, $\sin(\alpha/2) = \pm\sqrt{c/2a}$, and $\beta \equiv 0$. Note that sign "+" corresponds to the transfers via aphelion ("slow" transfers) and "−" to the transfer via perihelion ("fast" transfers).

3) If, moreover, the orbit is circular or if it is elliptical and its ending points are perihelion and aphelion then $r_1 + r_2 = 2a$, $\alpha = \pm\pi$, and again $t_n = nT/2$.

Of course, the same is true of every recurrent subitinerary extracted from the original itinerary.

Generally speaking, a transitional arc does not put any constraint on the flight time until the starting time and therefore the initial configuration of the planetary system is fixed. However, the first arrival at a planet in the itinerary defines a discrete set of recurrence opportunity times. In other words, every N-term itinerary comprising M planets may be decomposed into $M - 1$ transitive arcs and $N - M$ recursive trajectories, thus giving rise to $N - M$ synchronism conditions similar to Eq. (13). The decomposition can be fulfilled in a variety of ways subject to the connectedness condition of the corresponding graph [16]. Figure 4 presents a valid decomposition graph. An arbitrarily picked sample itinerary is {ABACBBCACBA}. Dashed and solid arcs denote transitive and recursive trajectories, respectively.

However, the decomposition has been done, given the durations of transitional transfers and the numbers of semirevolutions of planets over the recursive trajectories, absolute times τ_i of all GAMs are immediately available. They should form an increasing sequence. To satisfy this requirement, a set of simultaneous inequalities should be satisfied. Otherwise, one can sort τ_i in increasing order and correspondingly reorder GAMs in the itinerary. Now, flight times t_i over every arc are $t_i = \tau_{i+1} - \tau_i$. A unique trajectory is then defined by the set of natural numbers m_i of the spacecraft's semirevolutions supplemented with the signs $\sigma_i =$ " + " or "−" for fast and slow arcs. The extended notation of the preceding sample itinerary considered is

$$\{\mathrm{A}(t_1, m_1, \sigma_1)\mathrm{B}(t_2, m_2, \sigma_2)\mathrm{A}(t_3, m_3, \sigma_3)\mathrm{C}\ldots\mathrm{C}(t_9, m_9, \sigma_9)\mathrm{C}(t_{10}, m_{10}, \sigma_{10})\mathrm{A}\} \tag{15}$$

Now, equations identical to Eqs. (13) and (14) give the sought synchronism relations if n_i are replaced by m_i and the orbital elements (period and eccentricity) are those of the spacecraft over the arc under consideration. It should be emphasized that an extended itinerary might be inconsistent with the concatenation rules. It should be subject to the consistency proof. Let us consider two particular cases (E3BP and C4BP) in more detail.

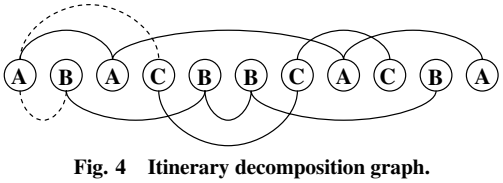

Fig. 4 Itinerary decomposition graph.

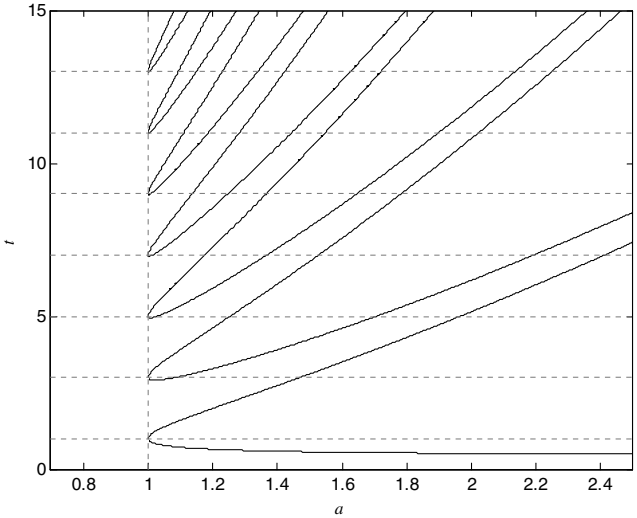

Fig. 5 Sample root lines of Lambert's equation (at $r_1/r_2 = 0.818$). Semimajor axes a are normalized to the planet's semimajor axis t to its orbital period.

D. Elliptical Three-Body Problem

In this case, all arcs are recursive. As will be later shown, the most efficient gravity-assist maneuvers take place at the planet's orbit apoapsis and periapsis. Consequently, the planet's transfer angle and time are $n\pi$ and $nT_{\mathrm{pl}}/2$, respectively; the spacecraft transfer angle is $m\pi$. Substituting these values into Eq. (13) results in the sought synchronism equation for the odd arcs (n and m are odd numbers):

$$(m-1)\frac{T}{2} \pm \frac{T}{2\pi}(\alpha - \sin\alpha) = (m-1)\frac{T}{2}$$
$$\pm \frac{T}{2\pi}\left[\sin^{-1}\sqrt{\frac{c}{2a}} + \sqrt{\frac{c}{a}\left(2 - \frac{c}{a}\right)}\right] = n\frac{T_{\mathrm{pl}}}{2} \tag{16}$$

Given the planetary orbit and therefore the radii r_1 and r_2, Eq. (16) can be solved *once* for the entire T/T_{pl} ratios. All solutions are presented in the well-known diagram [17], Fig. 5. The bottom branch corresponds to zero full revolutions of the spacecraft; every next (going up) branch adds one full revolution. Particular solutions at given combinations of n and m can be extracted from the plot. A trajectory that returns to the starting point in inertial space can be repeated after an adjustment of inclination for the sake of equalization of initial and final transversal velocities.

E. Circular Four-Body Problem

The next case is a particular case of recursive itineraries hereafter called *cycles*. These are the itineraries {ABB . . . BA}, with symbol A in the first and the last place only and symbol B in the remaining $N - 2$ places. All arcs except the first and the last ones are recursive. The respective flight times are

$$t_i = n_i T_B/2 \qquad (i = 2, \ldots, N-2) \tag{17}$$

The values of t_1 and t_{N-1} are arbitrary, though coupled by the relation

$$t_{N-1} = t_1 + n_A T_A/2 \tag{18}$$

Unlike the E3BP, a cycle in a general C4BP cannot be repeated because the configuration of the planetary system at the instant of the last GAM is not the same as at the first GAM. Yet, in a resonant

planetary system, the repetition is possible if the cycle duration is a common multiple of orbital periods of the planets. Note that the sequences $\{\tau_i\}$ are automatically monotonous in E3BP and C4BP cycles.

IV. Unidirectional GAM-induced Variation of V_∞

A. Mapping GAM Sequences

Considering the C4BP, every GAM near the first planet implies a change in $V_{\infty,2}$, the relative velocity near the second planet. Equivalently a GAM near the second planet implies a change in $V_{\infty,1}$, the relative velocity near the first planet. In the E3BP we get the same picture except for the fact that the GAMs are all relative to the same planet, albeit in its different locations. Therefore, in both cases, drawing the line of V_∞ changes in the $(V_{\infty,1}, V_{\infty,2})$ coordinate system, every GAM is mapped as a jump in the direction parallel to one of the coordinate axes. As a result, the chain of arcs looks like a staircase starting from initial values $[V_{\infty,1}(t_0), V_{\infty,2}(t_0)]$ and ending at final values $[V_{\infty,1}(t_f), V_{\infty,2}(t_f)]$ as shown in Fig. 6. Every vertical or horizontal line in this graph, for example segment AB, is a J variation during one cycle. We shall now derive the J variation during one cycle for the C4BP and E3BP.

B. J Variation During One Cycle

Let us consider a cycle in C4BP. The s/c is assumed to start from planet 1, with initial radial, transversal, and relative velocities, $V^-_{r,1}$, $V^-_{\theta,1}$, and $V^-_{\infty,1}$, respectively, and inclination angle i^-. Similarly X^-_2, X^+_2, and X^+_1 denote, respectively, the quantities at the first approach to planet 2, at the last departure from it, and at arrival back at planet 1. According to Secs. III.A and III.B, the participant variables obey the equation

$$\left(V^-_{\infty,1}\right)^2 = \left(V^-_{r,1}\right)^2 + \left(V^-_{\theta,1}\right)^2 + V^2_{\mathrm{pl},1} - 2V^-_{\theta,1}\cdot V_{\mathrm{pl},1}\cdot\cos i^- \quad (19)$$

and similar equations for X^-_2, X^+_2, and X^+_1. Besides, the following conditions are valid:

$$V^-_{r,1} = -V^-_{r,2} = V^-_r; \qquad V^+_{r,1} = -V^+_{r,2} = V^+_r \quad (20)$$

$$V^+_{\theta,2} = \frac{r_1}{r_2}V^-_{\theta,1}; \qquad V^-_{\theta,2} = \frac{r_1}{r_2}V^+_{\theta,1} \quad (21)$$

$$\left(V^-_{\infty,2}\right)^2 = \left(V^+_{\infty,2}\right)^2 = (V_{\infty,2})^2 \quad (22)$$

Equations (19–22) yield

$$\left(V^+_{\infty,1}\right)^2 - \left(V^-_{\infty,1}\right)^2 = \left(1 - \frac{V_{\theta,1}V_{\mathrm{pl},1}}{V_{\theta,2}V_{\mathrm{pl},2}}\right)\left[\left(V^+_r\right)^2 - \left(V^-_r\right)^2\right] \quad (23)$$

Because $V_{\mathrm{pl},j} = \sqrt{\mu/r_j}$, the sought formula for J variation during one cycle in the C4BP is given by

$$\frac{\left(V^+_\infty\right)^2 - \left(V^-_\infty\right)^2}{\left(V^+_r\right)^2 - \left(V^-_r\right)^2} = 1 - \left(\frac{c-r}{r}\right)^{3/2} \quad (24)$$

where r and $c-r$ are the distances from the sun to the first and second planets, respectively, $V^\pm_\infty$ are the s/c exchanged velocities relative to the first planet, and $V^\pm_r$ are the s/c radial velocities both at the start and end of the cycle.

Equation (24) holds in the case of the E3BP as well. Here, as already indicated, the GAMs occur at the apoapsis and the periapsis of the planets' orbit, where $V_{\theta,j} = V_{\mathrm{pl},j}$. In addition, $V_{\theta,1}/V_{\theta,2} = r_2/r_1$, due to momentum conservation. Substituting these values into Eq. (23) yields the formula for J variation in the E3BP case. Finally we can write the general equation of J variation during one cycle for both cases, C4BP and E3BP, as a single equation

$$\frac{\left(V^+_\infty\right)^2 - \left(V^-_\infty\right)^2}{\left(V^+_r\right)^2 - \left(V^-_r\right)^2} = 1 - \left(\frac{c-r}{r}\right)^q \quad (25)$$

where $q = 3/2$ for the C4BP, and $q = 2$ for the E3BP. In the E3BP, all relative values to first or second planets are replaced by values relative to the planet's orbital apoapsis and periapsis.

Equation (25) unambiguously defines the GAMs strategy for various mission goals. For example, in the E3BP, variation of the s/c radial velocity intended to increase J or V_∞ is $(V^+_r)^2 > (V^-_r)^2$ at the periapsis of the planet's orbit and $(V^+_r)^2 < (V^-_r)^2$ at the apoapsis, or vice versa for the opposite goal.

C. Optimal J Variation in Elliptical Three-Body Problem

We shall now show that in the E3BP, the most efficient gravity-assist maneuvers take place at the planet's apoapsis and periapsis where $V_{\mathrm{pl},r} \equiv 0$ and $V_{\mathrm{pl},\theta} \equiv V_\theta$. Effectively, substituting these values of the velocity components into Eq. (8) results in

$$V^2_\infty = V^2_r + 4V^2_\theta \sin^2\frac{i}{2} \quad (26)$$

Equation (26) applied to an arbitrary angle between LON and the apsidal points of a planet's orbit gives

$$V^2_\infty = (V_r - V_{\mathrm{pl},r})^2 + 4V^2_\theta \sin^2\frac{i}{2} \quad (27)$$

The same considerations as in Sec. IV.B result in

$$\left(V^+_\infty\right)^2 - \left(V^-_\infty\right)^2 = 4\mu(2r-c)(\cos i^+ - \cos i^-) \quad (28)$$

The relative velocity increment reaches its maximum value simultaneously with the distance separating the GAMs points, i.e., when the points belong to the planet's orbit line of apsides. The increment is zero, when the LON is perpendicular to the apsidal line $(c \equiv 2r)$.

D. Assembling a Trajectory from Blocks

The major difficulty in designing a long multi-GAM trajectory is the necessity of solving the synchronization problem after each GAM. However it is manageable when a planetary system periodically restores its configuration in inertial space. Obviously, a single-planet system returns to its initial configuration after every revolution of the planet. Moreover, examination of a table of orbital periods in the solar system [18] reveals that many of them are locked in resonance. The system restores after the minimal common multiple of periods of participant planets. The sought trajectory of the spacecraft must be in resonance with the planets. The proposed method is similar to the design of periodic trajectories, but with a gradual, monotonous J variation.

If a cycle is feasible, i.e., if it meets all concatenation and synchronization conditions, then *this same cycle simply rotated*

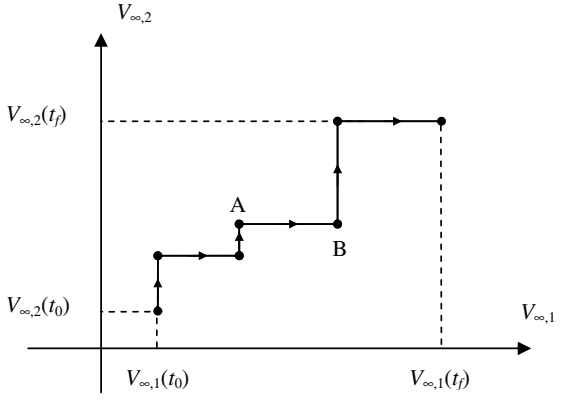

Fig. 6 V_∞ variation in the C4BP and E3BP.

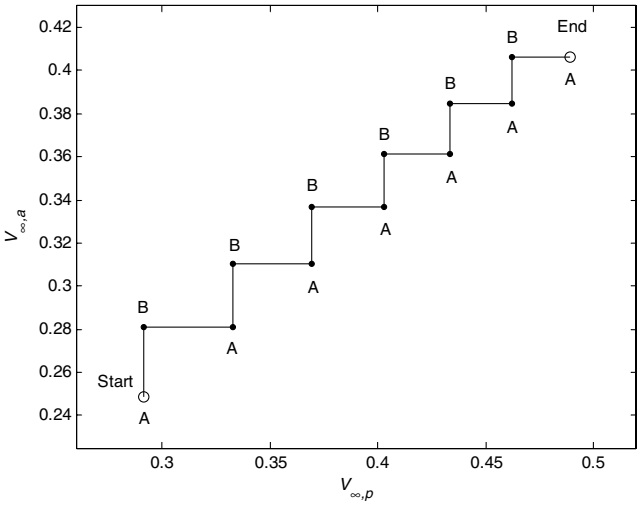

Fig. 7 V_∞ variation, the simplest one-cycle block.

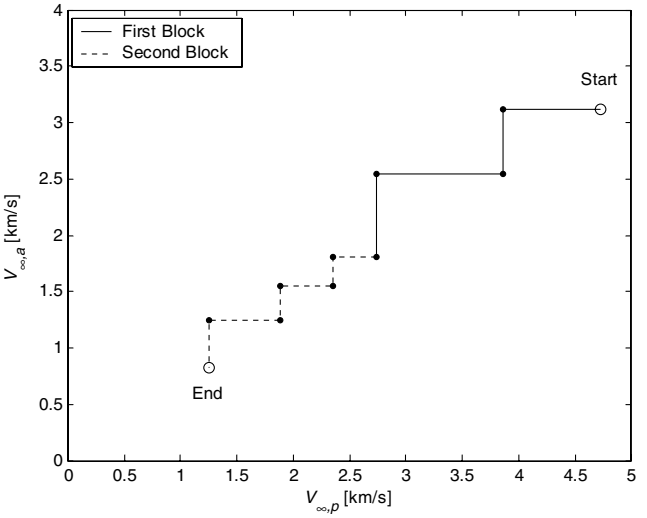

Fig. 8 V_∞ decrease in the sun–Mercury system.

about the LON is also feasible. The rotated cycle will provide a different value of J. Now if the configuration of the secondary bodies is the same at the end of a cycle as at the beginning, the same cycle may be repeated with a different inclination. Thus a cycle of out-of-plane arcs can be used as a block to build long trajectories, in particular those providing gradual monotonous J variation. Moreover, single blocks can be built from more than one cycle. If the total time of a sequence of cycles is a multiple of the resonant system period then the same sequence can be repeated with a different inclination, and therefore with a different J.

The E3BP gives a clear example of trajectory building from blocks. For simplification of the discussion, let us ignore for the moment the restriction on the maximal deflection angle of $\boldsymbol{V}_\infty$. Then any sequence of arcs meeting the synchronism condition can be combined in a block by linking an arc that returns the values of $T_{\rm pl}/T$ and n to their initial values to the end of the sequence. Figure 7 shows the V_∞ evolution in a coordinate system introduced in Sec. IV.A. The planet's orbit has an eccentricity of 0.1; the semimajor axis and gravity constant of the primary are normalized to one. The simplest block $\mathrm{A}\to\mathrm{B}\to\mathrm{A}$ consists of fast ($V_r=-0.12$) and slow ($V_r=0.26$) odd arcs. Initial values for V_∞ are $V_{\infty,p,0}=0.25$, $V_{\infty,a,0}=0.29$. In Fig. 7, the same block is implemented six times to increase V_∞.

Figure 7 clearly shows an important trend: the efficiency of the same block increases for a decreasing V_∞. This tendency is present in all classes of blocks. It can be easily derived from Eq. (26). This is why it is impractical to repeat a single block too many times. Moreover, sooner or later either the deflection angle of $\boldsymbol{V}_\infty$ will get beyond the maximal attainable value (appearing in the case of increasing J), or the inclination of an arc will vanish (in the case of decreasing J). Then a block should be replaced with a different one.

V. Representative Examples

A. Mercury Satellite Injection

In this example we consider the final stage of a Mercury mission. The ellipticity of Mercury's orbit will be used to decrease the spacecraft/Mercury relative velocity after the interplanetary transfer. Figure 8 and Table 1 present an example of the proposed strategy, when the s/c has already reached Mercury and a multi-GAM decreasing V_∞ is needed.

The trajectory starts from the perihelion of Mercury; the initial V_∞ is 4.7 km/s at the perihelion, the final position is the aphelion of Mercury's orbit, and the final V_∞ is 0.83 km/s. The trajectory is built from two blocks, one repeated twice and the other three times. Each block contains two odd arcs. Using the notation introduced in Sec. III.C, the trajectory can be presented as

$$\begin{aligned} &2\{P(0.5T,1,-)A(8.5T,17,+)P\},\\ &3\{P(0.5T,1,-)A(16.5T,33,+)P\} \end{aligned} \tag{29}$$

Here P and A denote the perihelion and the aphelion of Mercury's orbit, and T is its period. Every block is repeated until zero inclination is reached. These blocks were chosen to minimize the transfer duration. The blocks have the duration of 9 and 17 Mercury years. Therefore the total transfer time is 69 Mercury years, that is, about 16.6 Earth years. This long total transfer time is due to low values of V_∞ at the final stages of the transfer. It leaves no low-order synchronisms other than 1:1. Every block is repeated as long as the inclination angle is real and the turning angles of the velocity vector at GAMs are feasible.

Table 1 V_∞ decrease in the sun–Mercury system

Blocks	#	Position	Inclination angle, deg	V_∞, km/s	Closest approach distance, km	Arc TOF, Mercury's yrs
	——	P	4.6	4.7	——	0
$\{P(0.5T,1,-)A(8.5T,17,+)P\}$	1	A	2.95	3.11	637	0.5
		P	3.76	3.87	578	8.5
	2	A	1.3	2.55	95	0.5
		P	2.66	2.74	418	8.5
	1	A	1.95	1.8	9140	0.5
		P	2.28	2.35	8130	16.5
	2	A	1.39	1.55	8980	0.5
		P	1.83	1.88	9050	16.5
	3	A	0.24	1.24	4880	0.5
		P	1.22	1.25	5560	16.5
$\{P(0.5T,1,-)A(16.5T,33,+)P\}$	——	A	1.22	0.83	——	0.5

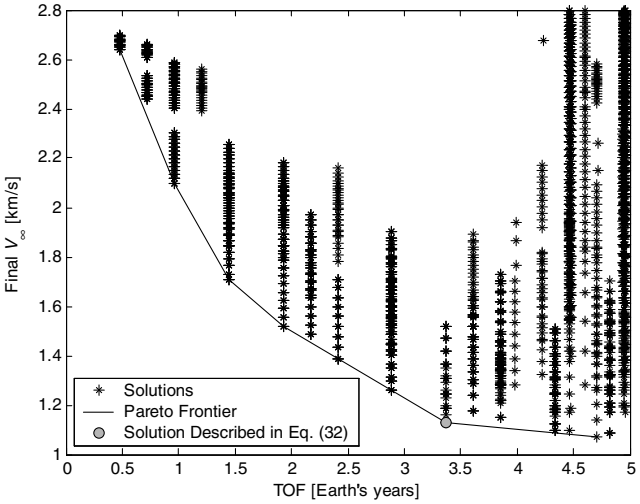

Fig. 9 E3BP trajectories attainable by variation of the LON direction and their Pareto frontier.

To reduce the total time transfer, we allow a small angle between the LON and the planet's apsidal line (θ_{LON}). Thus we worsen in the efficiency of J variation for *new synchronization options*. These stem from the difference between the durations of the planet motion along the two halves of its orbit. This doubles the number of synchronism options compared with that at $\theta_{\mathrm{LON}} = 0$. Equation (16) achieves the form

$$(m-1)\frac{T}{2} \pm \frac{T}{2\pi}\left[\arcsin\sqrt{\frac{c}{2a}} + \sqrt{\frac{c}{a}\left(2-\frac{c}{a}\right)}\right] = (n-1)\frac{T_{\mathrm{pl}}}{2} \pm \frac{T_{\mathrm{pl}}}{2\pi}\left[\arcsin\sqrt{\frac{c}{2a_{\mathrm{pl}}}} + \sqrt{\frac{c}{a_{\mathrm{pl}}}\left(2-\frac{c}{a_{\mathrm{pl}}}\right)}\right] \tag{30}$$

where

$$c = \frac{2p_{\mathrm{pl}}}{1-(e_{\mathrm{pl}}\cos\theta_{\mathrm{LON}})^2} \tag{31}$$

and signs on both sides of Eq. (30) are mutually independent. Many solutions to Eq. (31) fall within the interval of interest. All two-block trajectories with TOF shorter than 69 Mercurian years, available with free θ_{LON}, were computed. Figure 9 shows the solutions supplying the minimum final V_∞ at a given TOF. Initial V_∞ is always the same as in the previous example but now V_∞ is referred to the node located at θ_{LON}.

The itinerary below presents one of the trajectories depicted in Fig. 9 (gray dot). It requires $\theta_{\mathrm{LON}} = 18$ deg and yields $V_\infty = 1.13$ km/s after eight GAMs and 3.37 Earth years of flight vs 16.6 years in the previous example. Symbols P and A now denote the nodes closest to the perihelion and the aphelion, respectively.

$$3\{P(0.5T,1,+)A(2.5T,5,-)P\} \quad \{P(0.5T,1,+)A(4.5T,9,-)P\} \tag{32}$$

The transfers could be improved even more by applying small delta-V maneuvers provided by an onboard propulsion system but this issue is beyond the scope of this paper.

B. Ballistic Multi-GAM Trajectories in the Jupiter Galilean Moons System

In this section we present an example of a multi-GAM trajectory in a resonant system. The Galilean moons of Jupiter, Io, Europa, and Ganymede are in a 1:2:4 resonance. The trajectory proposed herein is linked from the trajectories in three two-moon resonant systems: Io–Europa and Io–Ganymede.

The trajectory starts from Io with V_∞ somewhat exceeding the minimum sufficient to reach Europa. The V_∞ is built up to a value, which enables a transfer from Io to Ganymede. The objective of the second phase is reaching Ganymede and synchronization with its orbital motion by matching the s/c orbital plane with the common orbital plane of the Jovian moons. The second phase is completed at the moment of the first encounter with Ganymede. At the third phase, V_∞ decreases up to the level enabling the Io-to-Callisto transfer, now in the Io–Ganymede system.

Given starting and destination planets in coplanar circular orbits, Hohmann's transfer has minimum V_∞ at the starting planet among all interception trajectories. Hohmann's Io–Europa trajectory has V_∞ near Io of 1.9 km/s; V_∞ of Io–Ganymede trajectory near Io is 3.4 km/s. Initial velocities of multi-GAM trajectories must exceed these values. Examination of available synchronisms at various θ_{IE} reveals a variety of arcs with $V_{\infty,I} = 2$ km/s and a short transfer time at $\theta_{\mathrm{IE}} = 51$ deg. The respective initial value of θ_{IG} is 114.7 deg. An example of the first phase trajectory (from Io to Europa) is presented by the itinerary

$$\{I(4.02,3,+)E(1.29,1,-)I\}, \qquad 8\{I(9.31,7,+)E(1.27,1,-)I\} \tag{33}$$

(times in this and the next itinerary are given in Earth days). Its duration is 90 days. Figure 10 presents the history of building up the approach velocities at Io and Europa. Note the variation of stair heights. The second phase trajectory contains even arcs only, namely those in resonance 4:7 and 1:2 with Io. The itinerary of the second phase is given by

$$\{I(12.39,8,+)I(3.54,2,+)I\} \tag{34}$$

Total TOF of the second phase is 15.9 days. It does not change V_∞ at Io but it does change the modulus of the spacecraft orbital velocity. Finally the spacecraft arrives at Ganymede. A GAM near it establishes the synchronism with its orbital motion. The third-phase trajectory (Io to Callisto) is built from four consequent arcs, the third repeated thrice and the fourth twice. It is given by the itinerary

$$\{I(2.25,1,+)G(18.9,9,-)I(2.25,1,+)G(31.24,15,-)I\} \quad 3\{I(3.54,4,+)I\}, \qquad 2\{I(14.58,7,+)G(6.57,3,-)I\} \tag{35}$$

The transfer takes in total 107.5 days. Figure 11 is analogous to Fig. 10. The total transfer time for such a mission is about 213.3 days. All flyby altitudes exceed 100 km, therefore the trajectory is a practical initial approximation to a real mission.

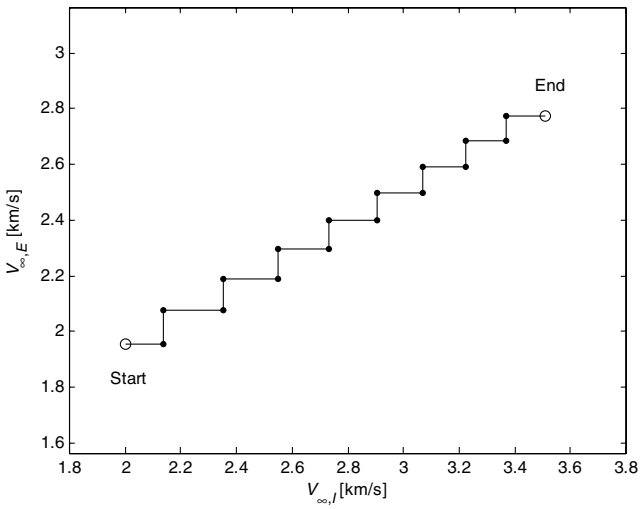

Fig. 10 Phase 1: V_∞ buildup in Io–Europa system.

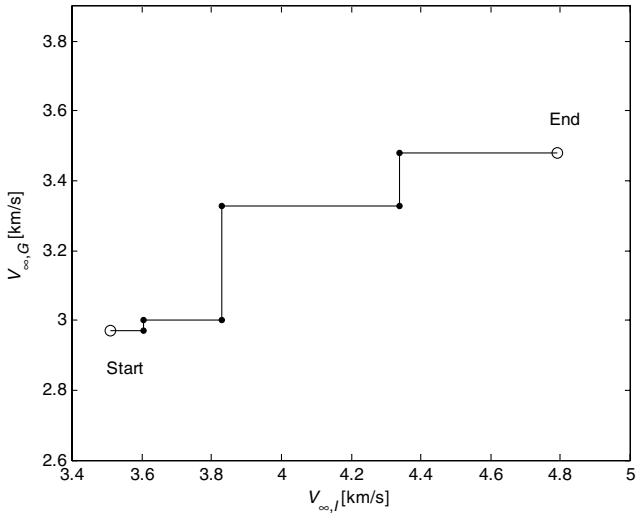

Fig. 11 Phase 3: V_∞ buildup in Io–Ganymede system.

VI. Conclusions

This paper presents a novel tool for efficiently building long interplanetary trajectories with multiple GAMs. We use the asymptotic case of the three-body problem where the mass of a body used for gravity-assisted maneuver tends to zero known as the collisional two-body problem. The orbits we use are built from non-coplanar arcs with angular distances of $k\pi$.

A regular method for building much longer multi-GAM trajectories was proposed. It is based on the repetitive use of identical subsequences (blocks) of flybys. Block building is a powerful method for synthesizing very long multi-GAM transfers in any E3BP or N-body resonant systems.

The only consumed resource at gravity-assisted maneuvering is time. We did not undertake any special effort toward the trajectory optimization. However the TOF obtained for different types of missions are obviously feasible. There is a possibility to further reduce TOF, performing discrete optimization with the aim of building optimal blocks and combining them into a long multi-GAM trajectory. In addition, the flight times attainable with multi-GAM trajectories can be reduced considerably by small assistance of low-thrust. These issues will be addressed in future papers.

References

[1] Murrill, M. B., "Grandest Tour: VOYAGER," *Mercury*, Vol. 22, No. 3, 1993, pp. 66–77.

[2] Diehl, R. E., Kaplan, D. I., and Penzo, P. A., "Satellite Tour Design for the Galileo Mission," AIAA Paper 83-101, Jan. 1983.

[3] Matson, D. L., Spliker, L. J., and Lebreton, J. P., "Cassini Huygens Mission to the Saturnian System," *Space Science Reviews*, Vol. 104, Nos. 1–4, 2002, pp. 1–58.

[4] Miller, J. K., and Weeks, C. J., "Application of Tisserand's Criterion to the Design of Gravity Assist Trajectories," *Aerospace Sciences Meeting and Exhibit*, AIAA Paper 2002-4717, Aug. 2002.

[5] Strange, N. J., and Longuski, J. M., "Graphical Method for Gravity-Assist Trajectory Design," *Journal of Spacecraft and Rockets*, Vol. 39, No. 1, Jan.–Feb. 2002, pp. 9–16.

[6] Petropoulos, A. E., Longuski, J. M., and Bonfiglio, E. P., "Trajectories to Jupiter via Gravity Assist from Venus, Earth, and Mars," *Journal of Spacecraft and Rockets*, Vol. 37, No. 6, 2000, pp. 776–783.

[7] Rinderle, E. A., "Galileo User's Guide, Mission Design System," Jet Propulsion Lab., California Inst. of Technology, Pasadena, CA, JPL D-263, July 1986.

[8] Sauer, C. G., "MIDAS: Mission Design and Analysis Software for the Optimization of Ballistic Interplanetary Trajectories," *Journal of the Astronautical Sciences*, Vol. 37, No. 3, July–Sept. 1989, pp. 251–259.

[9] Szebehely, V. G., *Theory of Orbits, The Restricted Problem of Three Bodies*, Academic Press, New York, 1967, pp. 83–136.

[10] Bruno, A. D., *Restricted 3-Body Problem: Plane Periodic Orbits*, Pt. 2, Walter de Gruyter and Co., Berlin, 1994, pp. 95–132.

[11] Battin, R. H., *Introduction to the Mathematics and Methods of Astrodynamics*, AIAA Education Series, AIAA, New York, 1987, pp. 264–265, 429–447.

[12] Hollister, W. M., "Periodic Orbits for Interplanetary Flight," *Journal of Spacecraft and Rockets*, Vol. 6, No. 4, 1969, pp. 366–369.

[13] Russell, R. P., and Ocampo, C. A., "Systematic Method for Constructing Earth-Mars Cyclers Using Free-Return Trajectories," *Journal of Guidance, Control, and Dynamics*, Vol. 27, No. 3, 2004, pp. 321–335.

[14] Russell, R. P., and Ocampo, C. A., "Global Search for Idealized Free-Return Earth-Mars Cyclers," *Journal of Guidance, Control, and Dynamics*, Vol. 28, No. 2, 2005, pp. 194–208.

[15] Bate, R. R., Mueller, D. D., and White, J. E., *Fundamentals of Astrodynamics*, Dover, New York, 1971, pp. 53–58.

[16] Tutte, W. T., *Connectivity in Graphs*, Toronto Univ. Press, Toronto, 1967, pp. 17–35.

[17] Eliasberg, P. E., *Introduction to the Theory of Flight of Artificial Earth Satellites*, Israel Program for Scientific Translations, Jerusalem, 1967, pp. 112–119.

[18] Alfven, H., and Arrhenius, G., *Evolution of the Solar System*, Scientific and Technical Information Office NASA, Washington, D.C. 1976, pp. 105–124.

D. Spencer
Associate Editor